

Exploring Thermoelectric Properties in Emergent Carbon Materials

Explorando Propriedades Termoelétricas em Novos Materiais de Carbono

Article Info:

Article history: Received 2023-10-01 / Accepted 2023-11-20 / Available online 2023-11-30

doi: 10.18540/jcecv19iss11pp17441



Lucas Lopes Lage

ORCID: <https://orcid.org/0000-0002-9085-0388>

Universidade Federal Fluminense, Brasil

E-mail: lucaslage@id.uff.br

Andrea Latgé

ORCID: <https://orcid.org/0000-0002-8152-6455>

Universidade Federal Fluminense, Brasil

E-mail: alatge@id.uff.br

Resumo

Desde a síntese do grafeno, diversos materiais com base em carbono previamente teorizados se tornaram alvo experimental de fabricação. Novos componentes passaram a ser explorados criando uma família de alótropos do grafeno, como os graphynes, metal organic frameworks (MOFs) e mais recentemente o biphenylene e seus derivados. Cada família possui sua particularidade com possíveis aplicações. Neste trabalho estudamos propriedades eletrônicas e de transporte desses materiais utilizando o modelo Tight-Binding e o formalismo de Landauer, a partir do cálculo das funções de Green. Os resultados para os coeficientes termoelétricos destes sistemas indicaram um alto potencial para aplicação em dispositivos nanoscópicos para reservar/produzir energia.

Palavras-chave: Alótropos. Grafeno. Propriedades. Termoelétricas. Dispositivos. Nanoscópicos.

Abstract

Since the graphene synthesis several theoretically predicted carbon based materials have become on the spot of experimental factories. Novel compounds were explored creating a family of graphene allotropes, such as graphynes, Metal Organic Frameworks (MOFs), and more recently biphenylene and its derivatives. Each family has its own particularity with possible applications. Here, the Landauer method with Green's function formalism was used within a Tight-Binding model to obtain electronic properties of such materials. The main results for the thermoelectric coefficients of such materials indicate a high potential application in nanoscopic devices to store/produce energy.

Keywords: Graphene. Allotropes. Thermoelectric. Properties. Nanoscopic. Devices.

1. Introduction

With the current environment crisis postponed by anthropological actions, new technology developments with either low emission rates and low environmental cost have become extremely important. In addition, the current computational capacity in front of Moore's law requires even more understanding and advancement in the study of nanodevice physics/chemistry (Poliakoff *et al.*, 2018). The 2-D materials showed as a prominent precursor to the development of new capable technologies to cope with such requirements. By graphite exfoliation A.Geim and K.Novoselov (Novoselov, 2004) were able to create an one-atom thick thin film called graphene [see Fig. 1(a)]. After that, several 2-D carbon-based materials (graphene allotropes) started to gain attention from the condensed matter community.

Some examples of 2D carbon (black dots) allotropes, that acquire visibility in this research field, are depicted in Fig.1 such as the Metal Organic Frameworks (MOFs) (Silveira, 2016) with a simplified kagome-honeycomb structure, shown in Fig.1-(b), which includes transition metal atoms (gray dots) between the carbons. The graphyne families in Fig.1-(c), are obtained by inserting acetylenic bonds (gray lines) inside the graphene hexagonal bounds in the case of α -graphyne, or between the hexagons, like in γ , β , (6, 6, 12)-graphyne (Baughman, 1987; Kang *et al.*, 2019), and other combinations namely graphdiyne (Fang *et al.*, 2022). Other examples depicted in Fig.1-(d) correspond to interplays between geometries, creating other unique properties, such as biphenylene (Fan *et al.*, 2021; Qitang *et al.*, 2021) and S-graphene (Bandyopadhyay *et al.*, 2020).

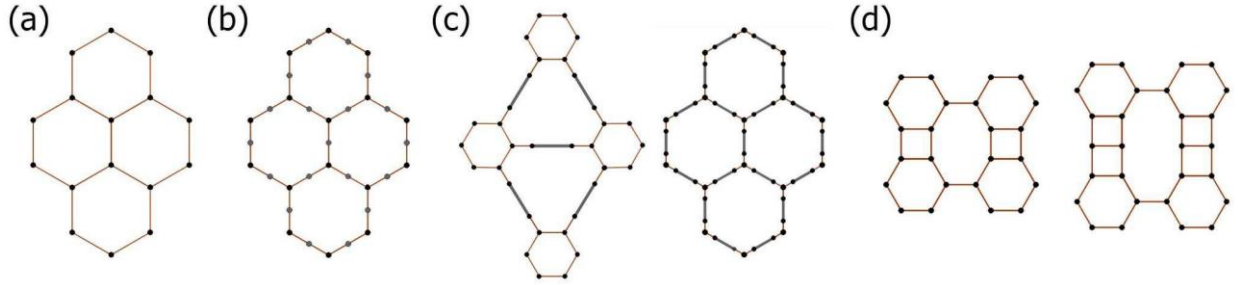


Figure 1 - (a) graphene, (b) kagomé honeycomb, (c) Left: γ -graphyne, Right: α -graphyne, (d) Left: biphenylene Right: S-graphene.

Alternative renewable energy production such those used from biomass, wind, and solar radiation is thermoelectricity (TE). Important in the storage and primary energy, the TE materials convert energy in temperature, and vice versa, via the Seebeck effect. The figure of merit (ZT) is a dimensionless quantity that measures the TE performance. Due to electron confinement, low dimension systems are supposed to increase the ZT as we will see for the proposed nanodevices, mainly for the materials with semiconducting nature (Finn, 2021).

2. Theory

A single-orbital tight-binding (TB) Hamiltonian is used to describe the systems studied, given by

$$H = \sum_i \varepsilon_i c_i^\dagger c_i + \sum_{\langle ij \rangle} t_{ij} c_i^\dagger c_j + \sum_{\langle\langle ij \rangle\rangle} t'_{ij} c_i^\dagger c_j + h.c. \quad (1)$$

with ε_i being the on-site energy for each atom located at site i , c_i^\dagger (c_i) is the creation (annihilation) operator of an electron confinement is characterized by Van Hove singularities site i , and t_{ij} and t'_{ij} are the hopping energies for nearest and second-nearest neighboring atoms, respectively.

Total end Local Density of states (DOS and LDOS) are calculated within the Green's function formalism. We also investigated transport properties using the Landauer approach (Data, 2014) in which the system is decoupled into three parts: central conductor and right and left leads (Chico *et al.*, 2015). We have considered semi-infinite leads, matching perfectly with the central region. The central advanced (a) and retarded (r) Green's functions are given by

$$G_c^{a,r}(E) = [w - H_c - \Sigma_L^{a,r}(E) - \Sigma_R^{a,r}(E)]^{-1}, \quad (2)$$

with $w = E \pm i\eta$, η being an infinitesimal number. H_c is the Hamiltonian of the central part, and $\Sigma_{L,R}^{a,r}(E)$ corresponds to left and right self-energies, given by the related surface Green's functions, from which the coupling matrices are obtained:

$$\Gamma^{L,R}(E) = i(\Sigma_{L,R}^r(E) - \Sigma_{L,R}^a(E)) \quad (3)$$

Finally, to derive the electronic conductance in nanoribbons, $G(E)=2e^2/h T(E)$ we calculate the energy-dependent transmission given by

$$T(E) = Tr[\Gamma^L G_c^r \Gamma^R G_c^a] \quad . \quad (4)$$

Once we get the electronic transmission $T(E)$, the electronic conductance $\sigma(\mu, T)$, Seebeck coefficient $S(\mu, T)$, power factor $P(\mu, T)$, and electronic thermal conductance $\kappa_e(\mu, T)$ can be obtained with the help of an integral function $Y_n(\mu, T)$ defined as (Wang *et al*, 2012)

$$Y_n(\mu, T) = \frac{2}{h} \int T(E)(E - \mu)^n [-\partial_E f(E, \mu, T)] dE \quad (5)$$

with $f(E, \mu, T)$ being the Fermi-Dirac distribution, μ is the chemical potential, and T the temperature. The coefficients $\sigma(\mu, T)$, $S(\mu, T)$, $P(\mu, T)$, and, $\kappa_e(\mu, T)$ can be derived as follows,

$$\sigma(\mu, T) = e^2 Y_0, \quad (6)$$

$$S(\mu, T) = -\frac{1}{eT} \frac{Y_1}{Y_0}, \quad (7)$$

$$P(\mu, T) = S^2 \sigma, \quad (8)$$

$$\kappa_e(\mu, T) = Y_2 - \frac{Y_1^2}{Y_0}. \quad (9)$$

Finally, we can obtain the ZT expression by using $ZT = \frac{\sigma S^2}{\kappa_e + \kappa_{ph}}$, where κ_{ph} is the phonon contribution that will be neglected in this work on the assumption that it does not strongly depend on energy and is considered small for the studied materials in this work (Wang *et al.*, 2012). The present ZT results, therefore, correspond to maximum estimations based on the quasi-static lattice scenario.

3. Results

By cutting the 2D material in one direction, quasi 1D nanoribbon systems are obtained with periodic boundary conditions along one direction and quantized in the other. As all considered systems are based on carbon hexagons, we adopt in this work the usual nomenclature Armchair (AGNR) and Zigzag (ZGNR) following the periodic direction defined on graphene, as shown in Fig.2(a).

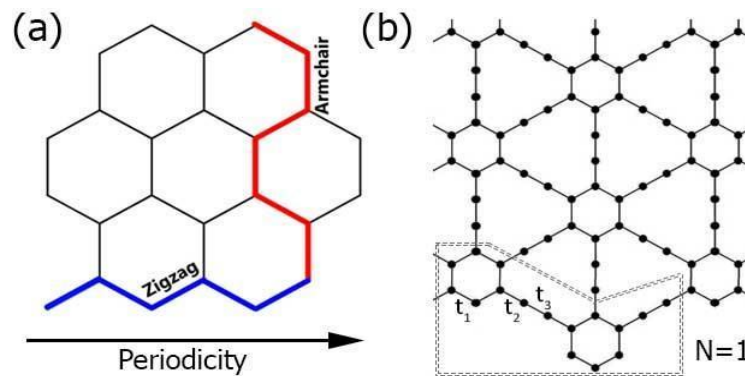


Figure 2 - (a) Periodic directions in graphene nanoribbons ZGNR and AGNR. (b) Comparison with γ -ZGyNR with the numeric unit cell delimited in the dashed area. With [$t_1 = -2.75$ eV, $t_2 = -2.63$ eV, and $t_3 = -3.25$ eV].

Each family system is directly connected with the geometries and symmetries of the unit cell in the 2D basis. This relation is crucial to determining the electronic properties of such systems as may be seen in Fig.3. The energy gaps for both armchair graphene nanoribbons (AGNR) and α -graphyne (α -AGyNR), are presented in Fig.3(a) and (b), respectively. The oscillatory pattern of metallic and semiconductor families reported in the literature for graphene nanoribbons are also exhibited here in the upper charts. The conductance of the α -AGyNRs have approximately the same channel numbers per energy as the AGNRs, ensuring hexagonal symmetry in both systems. Regarding the interest of creating a thermoelectric device, it is important to stress that semiconductor materials, as pointed out in the introduction, are the desired materials. In this particular case, our calculations (not showed here) pointed out that in comparison with the other graphynes and lattices proposed in this work, only the γ -graphyne is a semiconductor, as evidenced in Fig.4(1) and (2) at right, respectively, in both armchair and zigzag configurations, with bulk gap value $E_g = 0.5$ eV, consistent with the literature (Liu *et al.*, 2012). For this reason, all the following calculations are made exclusively for γ -graphyne features.

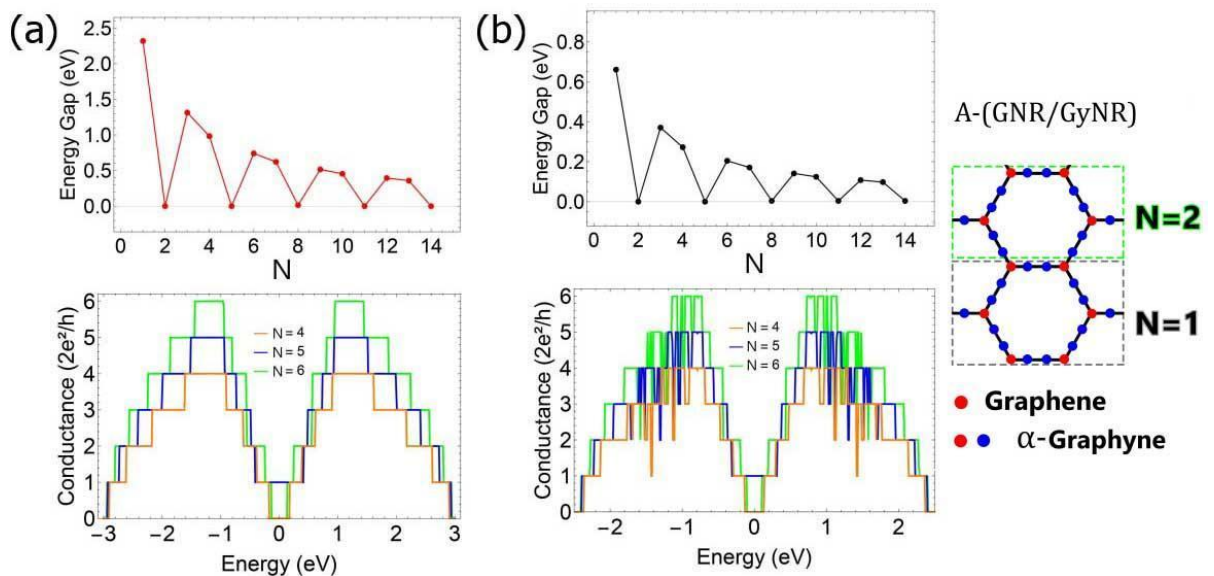


Figure 3 - Energy gap evolution and conductance for (a) AGNR [$t = -2.80$ eV] and (b) α -AGyNRs [$t_1 = -2.85$ eV (simple) and $t_2 = -7.50$ eV (triple)].

Fig.4 shows the thermoelectric coefficients for γ -ZGyNR. As expected, with temperature increasing, the conductance changes, reducing the channel amplitude values per energy, as depicted in Fig.4(a). A similar effect is shown for the Seebeck coefficient in Fig.4(b), where the global maximum is lowered for higher temperatures for a fixed nanoribbon size $N=2$. The results for the electronic thermal conductance and Seebeck are displayed in Fig.4(c) and (d), respectively, for room temperature ($T = 300$ K) and for several nanoribbon sizes. In both cases, the highest values for the $S(\mu, T)$ and $\kappa_e(\mu, T)$ are achieved for $0.2 \text{ eV} < \mu < 0.6 \text{ eV}$. This will be important for the figure of merit ZT in the following discussion. The power factor $P(\mu, T)$ of γ -ZGyNRs is shown in Fig.5. The main peak appears at $\mu = 0.5$ eV for the three values of temperature, with $N=2$ [left panel]. Otherwise, for $N=3$ and $T = 300$ K, [right panel] the main peak is located near $\mu = 0.45$ eV.

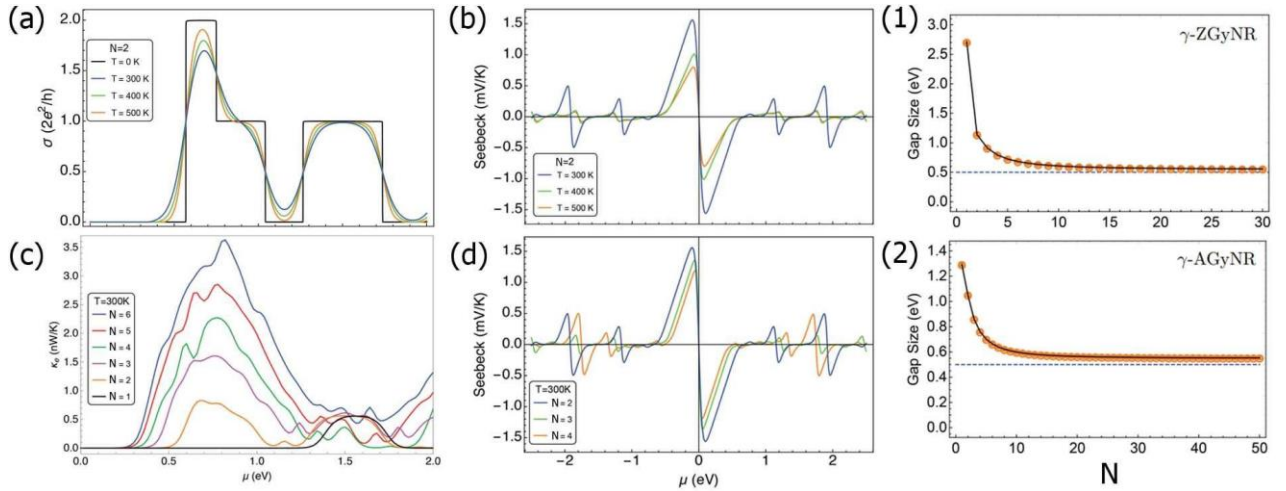


Figure 4 - Results for $N=2$ γ -ZGyNRs Conductance $\sigma(\mu, T)$ (a) and Seebeck coefficient (b) for different temperature values. (c) Electronic thermal conductivity and (d) Seebeck coefficient for different ribbon widths. (1) and (2) Energy gap evolution of Zigzag and Armchair features, respectively.

The ZT value for the γ -ZGyNR in this case is straightforwardly obtained by comparing the κ_e value in Fig.4(c) and the P value at the right panel of Fig.5, for this chemical potential value. We see that $\kappa_e(\mu = 0.45, T = 300) = 0.2$ nW/K and $P(\mu = 0.45, T = 300) = 17$ nW/K² in Fig.5, which gives an electronic $ZT = 85$. This is an excellent value for ZT, considering that the required performance for usual TE materials is $ZT = 3$ (Polozine, 2014). We conclude that γ -graphyne thin films are promising for applications in thermoelectric devices, since it has already been synthesized.

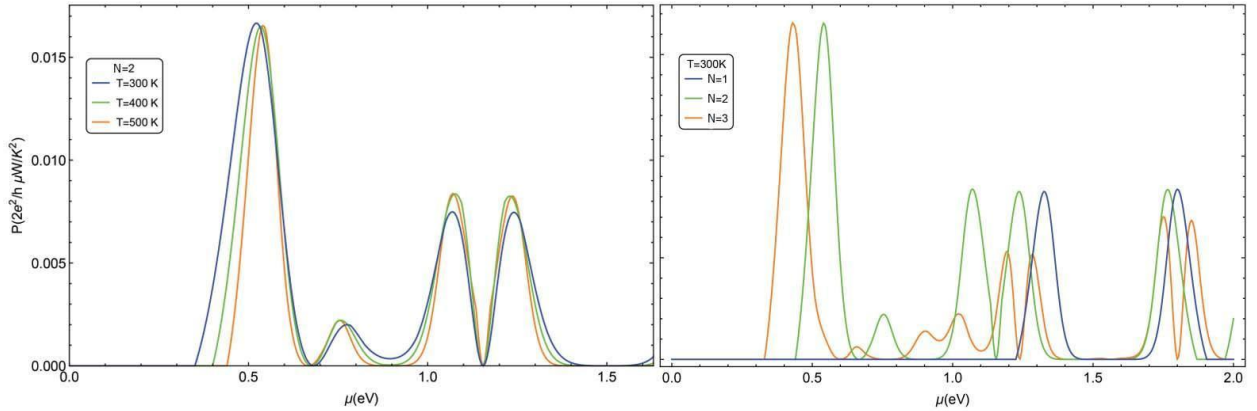


Figure 5 - Power factor ($P = \sigma S^2$) of γ -ZGyNR as a function of the chemical potential μ (eV). Left: Fixed size $N=2$. Right: Fixed Temperature $T=300$ K.

In the following, we perform the thermoelectric calculations for the biphenylene nanoribbons and compare the electronic bands with Density-functional theory (DFT). On the top part of Fig.6(a) we can see that the system is predicted to have a Dirac Cone Type-2 between the $Y - \Gamma$ path, in both DFT (blue dots) and TB calculations. In Type-2 Cones, the tangent line along k direction, have the same sign. The 2D system is metallic, as evidenced on bottom of Fig.6(a), by the crossing energy levels in the DOS around the fermi energy $E_f = -1.98$ eV. Fig.6(b) presents the eigenenergy surface plot of the biphenylene system. In the unit cell shown in Fig.6(c) the hopping parameters between the atomic sites, t_1, t_2, t_3, t_4, t_5 and t_6 , are represented by the colored lines, black, green, red, grey, magenta, and blue, corresponding to the distances 1.4 Å, 1.45 Å, 2.05 Å, 2.29 Å, 2.53 Å, 2.72 Å, respectively, chosen in the model to better fit DFT results. We have mapped the hopping energies by $t' = t_1 \cdot \exp[\beta(1 - r_{ij}/1.40)]$ (Suárez, 2011), with $\beta = 3$, $t_1 = -2.95$ eV, and the distances r_{ij} in the range 1.40-3.44 Å.

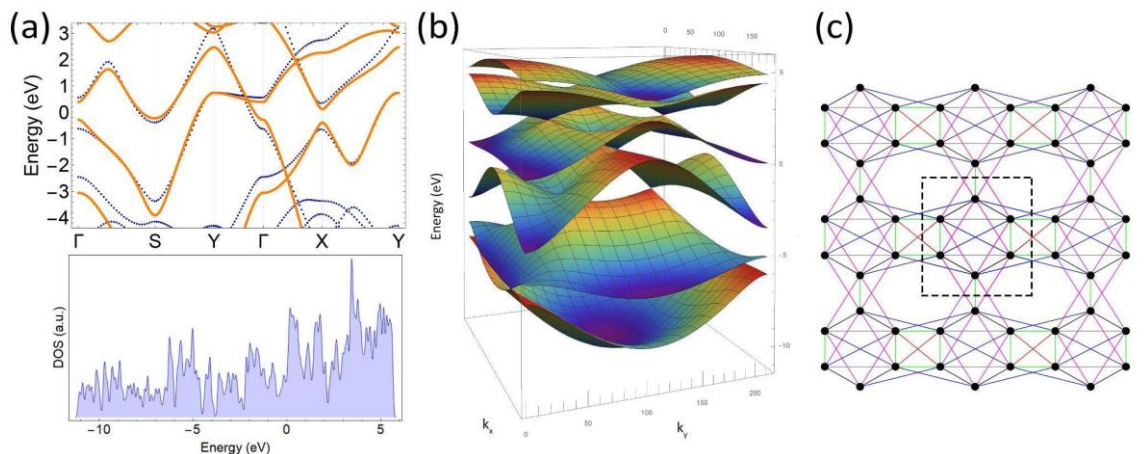


Figure 6 - (a) Top: Orange and blue dots, TB and DFT results for 2-D biphenylene, respectively. Bottom: Respective Density of states (DOS) calculated with TB. (b) Surface energy bands dispersion in function of k_x and k_y . (c) Real space unit cell, with colors representing the hopping and on-site energy $\varepsilon = -1.35$ eV.

Besides the metallic bulk of 2D biphenylene, we have also investigated the Armchair nanoribbons (AByNR), synthesized recently (Fan et al, 2021). As illustrated in Fig.7, the AByNRs show a semiconducting nature for small widths, with a small energy gap that quickly goes to zero at the fermi-level ($E = 0$ eV), as expected because of the bulk properties (see Fig.6). We notice that our TB calculations (orange curves) are in good agreement with the DFT calculations (black curves). The unit cell of a 5-AByNR is depicted on the right side, where the black, red, and green lines indicate the hoppings t_1 , t_2 and t_3 , respectively. As predicted by both models, all nanoribbons wider than the corresponding to $N=5$ are metallic.

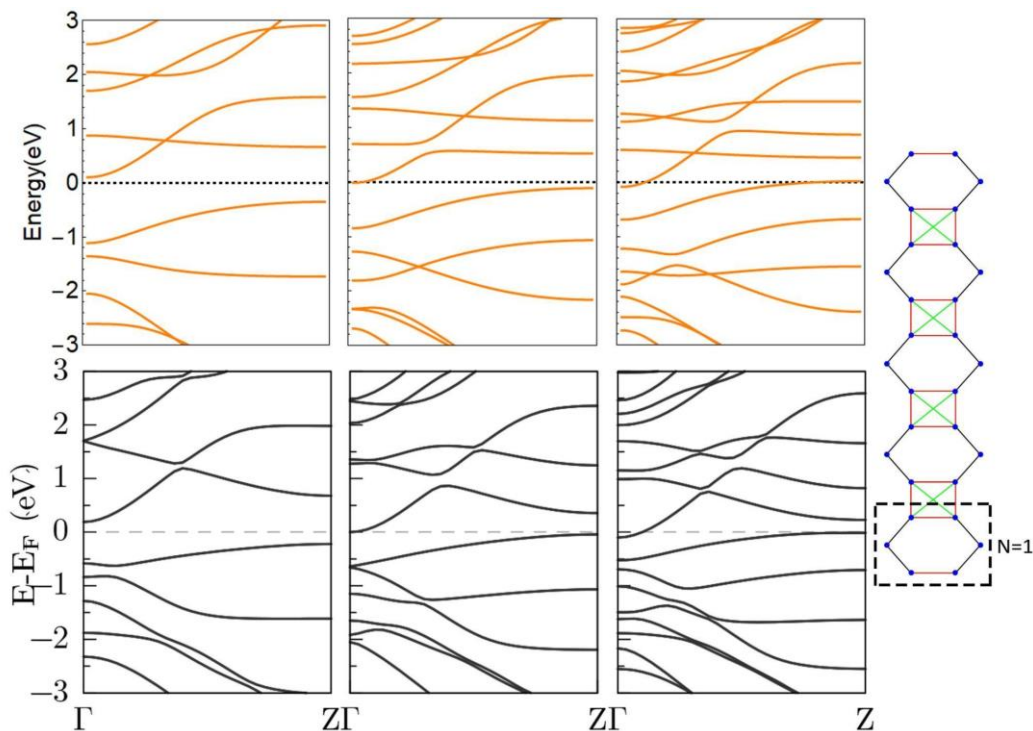


Figure 7 - TB (top) and DFT (bottom) electronic band structures for N -AByNR, with $N=3, 4$, and 5 , from left to right. At right: 5-AByNR; black dashed region encloses the unit cell for $N=1$. Black, red and green lines correspond to different hopping energies $t_1 = -2.75$ eV, $t_2 = -2.55$ eV, and $t_3 = -0.8$ eV. Blue dots denote on-site energies $\varepsilon = -0.5$ eV.

An interesting aspect about the biphenylene nanoribbons is the fact that small thin films experimentally synthesized by a Germany group (Fan et al, 2021) revealed the semiconducting character predicted in both theoretical descriptions. Therefore, we analyze the thermoelectric properties of the system, as shown in Fig.8.

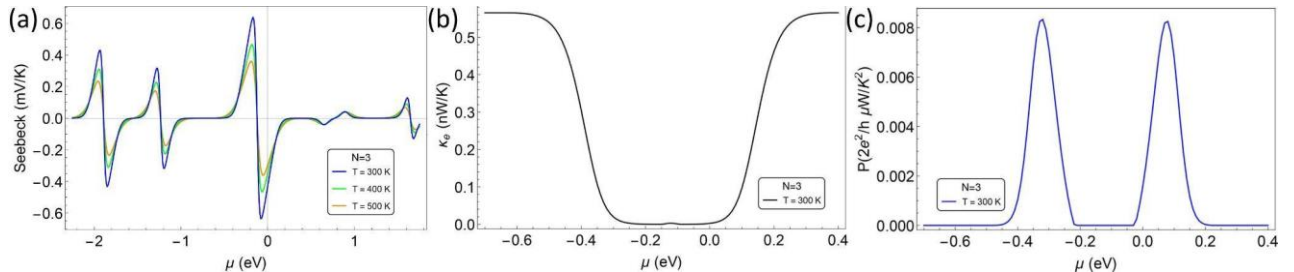


Figure 8 - Thermoelectric coefficients for a 3-AByNR: (a) Seebeck, (b) Electronic thermal conductance, and (c) Power factor.

Besides the smaller size of the 3-AByNR in comparison with the 3- γ -ZGyNR, which in theory could enhance the Seebeck coefficient, we notice in Fig.8(a) that the Seebeck peaks reach minor values near the inflection point in comparison with the previous results for the other nanoribbon families. Comparing the $\kappa_e(\mu = -0.35, T = 300) = 0.1$ nW/K with $P(\mu = -0.35, T = 300) = 6$ nW/K² in Fig.8(b) and (c), respectively, we obtain an electronic $ZT = 60$ which is smaller in contrast with the previous 3- γ -ZGyNR, although still a high value for ZT . As mentioned before, all the ZT values may be viewed as overestimated results, due to the missing lattice contribution.

4. Conclusion

We conclude that due to the rich chemical versatility of Carbon, it is possible to create new materials with different properties that can be used to guide technological advances. Here in this work, we showed a brief potential application of some of those materials denominated graphene allotropes, being created by inserting triple bounds between the graphene hexagons, generating the graphynes, or by including different geometries between those hexagons, leading to biphenylene, and other composites. We have performed electronic properties calculations of γ -graphyne and biphenylene nanoribbons and applied it to thermoelectric potential devices. Both armchair and zigzag γ -GyNRs are shown to be semiconducting materials with $E_g = 0.5$ eV, while the α -GyNRs follows the same gap profile of GNRs, being metallic for zigzag, and alternating between metallic and two semiconductor families for armchair in small sizes and going to null gap configuration when the system is sufficiently large.

For the biphenylene, we verified (not showed here) that the ZByNRs are always metallic, as the ZGyNRs, and present semiconducting character for small sizes of AByNRs, going to null gap as the ribbon width increases, as expected for the 2D counterpart systems. Concerning thermoelectric properties, due to the high ZT values for both studied systems in comparison with graphene samples, they showed to be promising materials to produce clean energy in the near future.

Acknowledgements

AL and LLL would like to thank the Brazilian Agencies CNPq, CAPES, FAPERJ. The DFT results were obtained in collaboration with Prof. Padilha from UFPR (Universidade Federal do Paraná) and Olga Arroyo Gascón from UCM (Universidad Complutense de Madrid).

References

- Bandyopadhyay, A. et al. (2020). The topology and robustness of two Dirac cones in S-graphene: A tight binding approach. *Scientific Reports* volume 10, 2502. <https://doi.org/10.1038/s41598-020-59262-2>
- Baughman, R. H., Eckhardt, H., Kertesz, M. (1987). Structure-property predictions for new planar forms of carbon: Layered phases containing sp² and sp atoms. *J. Chem. Phys.* 87, 6687–6699. <https://doi.org/10.1063/1.453405>.
- Chico, L., Latge, A. and Brey, L. (2015). Symmetries of quantum transport with Rashba spin–orbit: graphene spintronics. *Phys. Chem. Chem. Phys.* 17, 16469. <https://doi.org/10.1039/C5CP01637A>.
- Datta, S. (2014). *Electronic Transport in Mesoscopic Systems*. Cambridge University Press; Revised edition.
- Fan, Q. et al. (2021). Biphenylene network: A nonbenzenoid carbon allotrope. *Science* 372, 6544. *Science*, Vol 372, Issue 6544, pp. 852-856, <https://doi.org/10.1126/science.abg4>.
- Finn, P. A., Asker, C., Wan, K., Bilotti, E., Fenwick, O., Nielsen, C. B. (2021). Thermoelectric Materials: Current Status and Future Challenges. *Front. Electron. Mater* 1, 677845. <https://doi.org/10.3389/femat.2021.677845>.
- Gao, X., Liu, H., Wang, D. and Zhang, J. (2019). Graphdiyne: synthesis, properties, and applications. *Chem. Soc. Rev.*, 2019,48, 908-936. <https://doi.org/10.1039/C8CS00773J>.
- Haldane, F. D. M. (1988). Model for a Quantum Hall Effect without Landau Levels: Condensed-Matter Realization of the “Parity Anomaly”. *Phys. Rev. Lett.* 61, 2015. <https://doi.org/10.1103/PhysRevLett.61.2015>.
- Kang, J., Wei, Z., and Li, J. (2019). Graphyne and Its Family: Recent Theoretical Advances. *ACS Appl. Mater. Interfaces*, 11, 3, 2692–2706. <https://doi.org/10.1021/acsami.8b03338>.
- Liu Z. et al. (2012). A simple tight-binding model for typical graphyne structures. *New J. Phys.* 14, 113007. <https://doi.org/10.1088/1367-2630/14/11/113007>.
- Luo, Y., Ren, C., Xu, Y. et al. (2021). A first principles investigation on the structural, mechanical, electronic, and catalytic properties of biphenylene. *Sci Rep* 11, 19008. <https://doi.org/10.1038/s41598-021-98261-9>
- Morell, S. E., Vargas, P., Chico, L. and Brey, L. (2011). Charge redistribution and interlayer coupling in twisted bilayer graphene under electric fields. *Physics Review B* 84, 195421. <https://doi.org/10.1103/PhysRevB.84.195421>.
- Novoselov, K.S., Geim, A.K., Morozov, S.V., Jiang, D., Zhang, Y., Dubonos, S.V., Grigorieva, I.V., Firsov, A.A. (2004). Electric field effect in atomically thin carbon films, *Science* 306, 666–669. <https://doi.org/10.1126/science.1102896>.
- Poliakoff, M., Licence, P., George, M. W. (2018). A New Approach to Sustainability: A Moore's Law for Chemistry. <https://doi.org/10.1002/anie.201804004>.
- Polozine, A., Sirotinskaya, S., Schaeffer, L. (2014). History of development of thermoelectric materials for electric power generation and criteria of their quality. *Mat. Res.*17, 5. <https://doi.org/10.1590/1516-1439.272214>.
- Silveira, O. J., Alexandre, S. S., and Chacham, H. (2016). Electron States of 2D MetalOrganic and CovalentOrganic Honeycomb Frameworks: Ab Initio Results and a General Fitting Hamiltonian, *J. Phys. Chem. C* 120, 19796. <https://doi.org/10.1021/acs.jpcc.6b05081>.
- Wang, C. et al. (2012). Thermoelectric properties of gamma-graphyne nanoribbon incorporating diamond-like quantum dots. *Journal of Physics D: Applied Physics* 49, 135303. <https://doi.org/10.1088/0022-3727/49/13/135303>.